Extraordinary temperature amplification in ion-stimulated surface processes at low energies

Z. Wang and E. G. Seebauer*
Department of Chemical Engineering, University of Illinois, Urbana, Illinois 61801
(Received 17 September 2002; published 20 November 2002)

Molecular dynamics simulations of low-energy noble-gas atoms impacting Si and Ge surfaces reveal a new, unexpectedly strong trade-off between the energy threshold for point defect formation and substrate temperature. Nonuniformities in the net surface potential induced by thermal vibrations dramatically affect the locality of momentum transfer to the surface, thereby amplifying the effect of temperature by several orders of magnitude. This amplification may offer a new means for selecting specific elementary rate processes during plasma processing or ion-beam-assisted deposition.

DOI: 10.1103/PhysRevB.66.205409 PACS number(s): 68.35.Fx, 34.50.Dy, 82.20.Wt, 82.65.+r

Ion surface interactions at low energies (<100 eV) characterize an increasingly diverse array of material processing steps in ion-beam-assisted deposition (IBAD), plasma-enhanced deposition, reactive ion etching (RIE), and other applications. The overall process behavior in these applications often reflects a delicate balance among several competing kinetic effects. In IBAD, for example, enhanced surface diffusion improves film properties, while defect formation, substrate sputtering, and embedding of the bombarding gas often degrade them.[1,2] Similarly, in RIE a transition between net deposition and net etching can take place in a way determined by the balance among ion sputtering, thermal desorption, surface diffusion, radical adsorption, and other temperature-dependent phenomena.[3,4]

The governing kinetic phenomena in such applications are often tacitly considered to lie at one of two poles: physical effects where momentum matching dominates[5] and chemical effects involving thermal activation of atomic bonds according to Arrhenius expressions. Despite some early, largely forgotten evidence to the contrary,[6] this dichotomy has rested secure for several decades. The dichotomy probably originates from the fact that most experimental and computational work has been done at ion energies greater than 100 eV, where projectile energies are much greater than thermal energies. Some recent work with ion energies at tens of eV has begun to recognize synergy between ion energy and substrate temperature[7–9] in influencing surface rate phenomena. However, the dynamics of such synergy has remained unclear.[9] Despite occasional cautions to the contrary,[10,11] there has been little explicit recognition that the two poles may be linked by a continuum over which physical and chemical effects become inextricably intertwined.

In this context, our group recently reported the first direct measurements of ion-influenced surface diffusion of Ge on Si(111).[12,13] Although conventional Arrhenius behavior adequately represented diffusion below ion energies of 65 eV, the Arrhenius parameters themselves depended nonlinearly on both ion beam characteristics and substrate temperature T. In particular, the energy threshold for the onset of ion influences depended upon T, increasing discontinuously for Ar^+ from 15 eV below roughly 1025 K to 25 eV above that temperature. At the low ion fluxes employed ($\sim 10^{12}$ ion/cm^2 s), direct ion-driven motion of mobile atoms cannot account for the observations;[13] ion-induced formation of surface point defects seems to dominate. Note, however, that the thermal kinetic energies of the surface atoms in these experiments lie near 0.1 eV, while threshold kinetic energies of the ions lie more than two orders of magnitude higher. If forming surface defects results from a simple combination of the ion and target atom kinetic energies, the observed trade-off between T and the energy threshold is nearly as anomalous as a mouse counterbalancing an elephant on a seesaw.

In an attempt to explain the anomaly, we report here the results of molecular dynamics (MD) simulations concerning ion-induced point defect formation. Although there exists a substantial MD literature on this subject,[14–18] to our knowledge there is no work describing the strong amplification of temperature reported here, particularly with the simple functional form we observe.

MD simulations of noble-gas bombardment of Si and Ge (111) surfaces were performed with a revised and updated version of a code we have used previously.[19] The ensemble included five mobile layers of 224 atoms each, resting upon 3 fixed layers. Si and Ge self-interactions were governed by Stillinger-Weber potentials,[20] while the universal potential[21] governed interactions between bombarding noble-gas atoms and Si or Ge. Ions impinged at an angle 60° off normal along the $[\bar{2}11]$ direction, which is perpendicular to one of the rows of closest packing in the hexagonal atom arrangement. Simulations proceeded for a period of 500 time steps (1.5 ps), which tests determined was long enough to observe point defect formation, but not sufficiently long to result in conventional thermal effects due to heating of the ensemble (which evolved adiabatically and therefore heated significantly upon thermalization of the incident energy). To improve counting statistics, we employed volleys of six regularly spaced impacting atoms per simulation. The energy transfer dynamics of individual impacts was examined in detail to assure that each impact remained independent of the others over the time scale of the simulation. At the end of each simulation, we recorded the per-impact probability of adatom formation, knock-in, sputtering, and bulk vacancy formation. Variation of the time step and number of mobile layers showed that the values chosen were adequate to avoid artifacts associated with temporal discretization and ensemble size.

Figure 1 shows typical per-impact probabilities as the ion

 ©2002 The American Physical Society

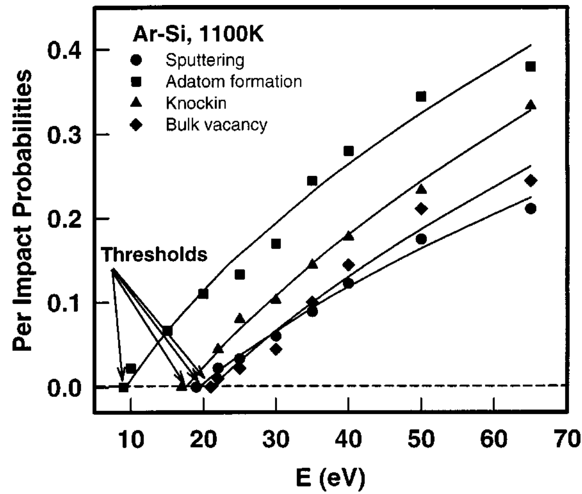

FIG. 1. Energy dependences of per-impact probabilities for various surface and bulk processes during Ar^+ bombardment of Si at 1100 K.

energy varies at a constant temperature T of 1100 K. For all four processes examined, the dependence on energy E was fit using the phenomenological square-root dependence $E^{1/2} - E_{\text{thres}}^{1/2}$. This form was chosen based on its well-documented use for ion sputtering[1,2] and because for each process this form best fits the data considered in aggregate over the various temperatures, substrates, and ion masses examined. Extrapolating this form via back to the horizontal axis via nonlinear least-squares fits yields threshold energies E_{thres} of 9 ± 2, 18 ± 1, 19 ± 1, and 21 ± 1 eV for adatom formation, knock-in, sputtering, and bulk vacancy formation, respectively.

Figure 2 shows similar per-impact probabilities for sputtering as T varies at constant ion energy of 65 eV. The effects of T exhibit are clearly large above a threshold temperature near 380 K. When the above-threshold probabilities were considered in aggregate over various ion energies, substrates, and ion masses examined here, the probabilities best obeyed a linear functional form. Extrapolation of this form to the horizontal axis yields a threshold T_{thres} of 384 ± 40 K. Plots similar to Fig. 2 characterize adatom formation, knock-in,

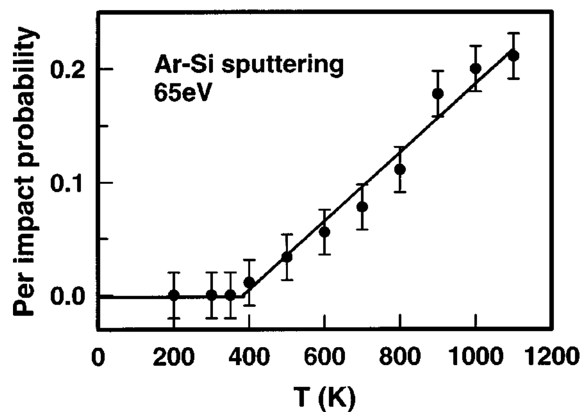

FIG. 2. Temperature dependence of per-impact sputtering probability during Ar^+ bombardment of Si at 65 eV.

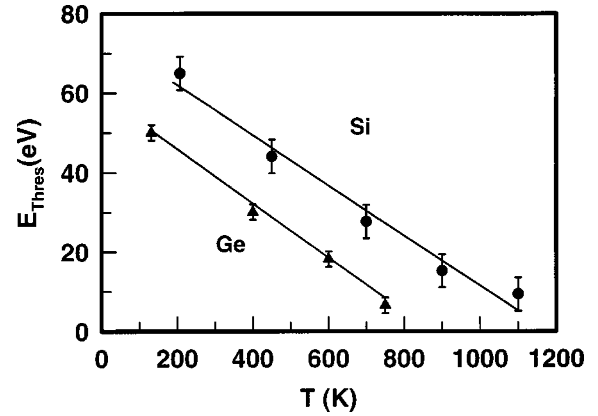

FIG. 3. Dependence of threshold energy upon temperature for Si and Ge adatom formation bombarded with Ar ions. The dependence obeys the relation $E_{\text{thres}} + \sigma kT = E_{\text{tot}}$, where σ and E_{tot} are constants.

and bulk vacancy formation, with T_{thres} lying at 200, 307, and 448 K. Uncertainties are also roughly ± 40 K.

We performed simulations of these kinds over a range of conditions sufficient to determine how E_{thres} varies with T for the four processes examined. Figure 3 shows example results for adatom formation. E_{thres} decreases strongly as T increases. Analogous data for the other three processes exhibit similar behavior. There is no theory available to suggest a functional form relating E_{thres} and T. However, a linear relation adequately describes the data set for each process, and this form best describes all data sets considered in aggregate. This form can be written as

$$E_{\text{tot}} = \sigma kT + E_{\text{thres}}, \tag{1}$$

where E_{tot} and σ denote constants and k represents Boltzmann's constant. We found that the parameter σ is large (700 ± 100) and identical to within statistical error for all four processes. E_{tot} exhibits more variation, lying at 77 ± 3, 81 ± 9, 97 ± 12, and 92 ± 11 eV for adatom formation, knock-in, sputtering, and bulk vacancy formation, respectively.

Figure 4 shows the variation of σ and E_{tot} for sputtering with ion masses corresponding to Ne, Ar, and Xe. Both σ and E_{tot} are rather insensitive to the identity of the bombarding atom for all four processes. Again, there is no theory available to use as a basis for functional form, so Fig. 4 simply employs phenomenological linear fits. Although the error bars in the slopes in Fig. 4 do not quite include zero (meaning no dependence on ion mass), comparable results for some of the other processes like sputtering do include zero as shown in Fig. 5. This insensitivity accords with a largely forgotten experiment performed 40 years ago[6] in which sputtering thresholds for a wide variety of solid elements were found to be largely independent of the mass ratio between impacting and substrate atoms in the energy range 35–300 eV. Figure 4 shows these results for both Si and Ge. Although σ does not depend significantly on the identity of the substrate, E_{tot} decreases from Si to Ge, with the ratio $E_{\text{tot,Si}}/E_{\text{tot,Ge}}$ being 1.46, 1.26, 1.36, and 1.37 for adatom formation, knock-in, sputtering, and bulk vacancy formation,

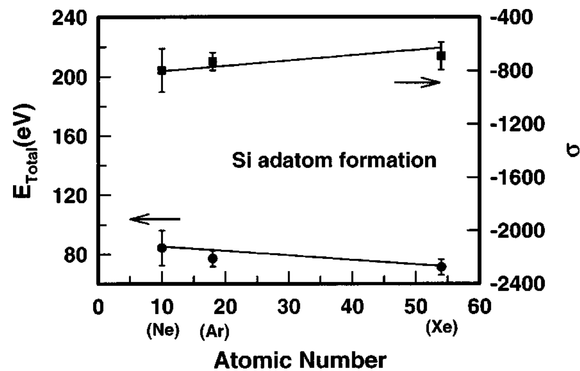

FIG. 4. Ion mass dependence of σ and E_{tot} for Si adatom formation. The mass dependence of both parameters is weak. The lines can be fit with a slope of 4.0 ± 2.2 for σ and -0.30 ± 0.18 for E_{tot}, where the error bars in this and the following figure have been calculated using statistical methods to account for variable error bars in the constituent data.

respectively. These ratios fall close to the ratio of cohesive energies $E_{coh,Si}/E_{coh,Ge}=1.20$ and the ratio of melting temperatures $T_{melt,Si}/T_{melt,Ge}=1.40$.

Equation (1) describes a nearly perfect trade-off between the threshold energy and surface temperature, with the effects of thermal energy amplified far beyond what one might normally expect. The form of Eq. (1) suggests that E_{tot} scales with the minimum energy that needs to be injected into the substrate in order to create a defect of a particular type. E_{tot} is almost certainly not equal to this minimum, since the simulations showed that the impinging atom typically deposits only about 40% of its energy into the substrate—the rest being carried off by the original projectile (which almost always reflects from the surface). However, the close relation between E_{tot} and the minimum energy we hypothesize is also supported by the way E_{tot} scales with substrate cohesive energy and melting temperature, which are both taken as proxies for defect formation energies. More support comes from the manner in which E_{tot} increases as the energy for point defect formation increases. Bulk vacancies require more energy to form than surface adatoms, for example, in accordance with the trend for E_{tot}. If the average energy carried off by the impinging atom is subtracted from E_{tot}, then the

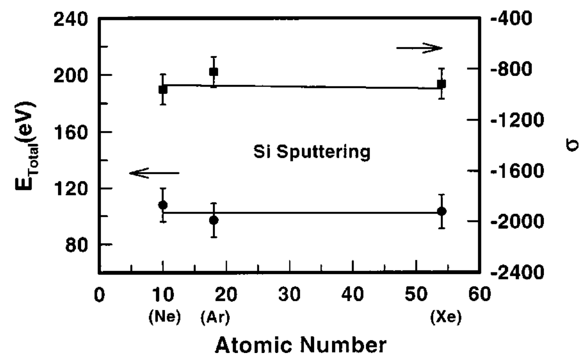

FIG. 5. Ion mass dependence of σ and E_{tot} for Si sputtering. The mass dependence of both parameters is weak. The lines can be fit with a slope of -0.67 ± 3.57 for σ and -0.01 ± 0.23 for E_{tot}.

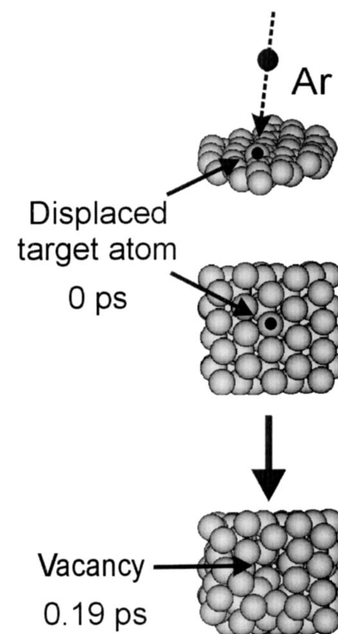

FIG. 6. Ion energy of 30 eV and temperature of 1100 K. Because the target atom (marked with a black dot) resides nearly 0.3 Å from its lattice site at the instant of impact due to thermal vibrations, defect formation takes place. No defect would have formed in the absence of such a significant excursion.

minimum energy for defect formation varies between 31 and 37 eV, depending on the particular defect being created.

Qualitative examination of molecular dynamics movies provided insight into why σ is so large. We found that at E-T conditions near the threshold for defect formation, the instantaneous position of the target atom is very important. If the target atom lies very near its lattice site, no defect forms and the impinging ion reflects nearly specularly. However, if thermal motions have caused the target atom to deviate 0.3–0.4 Å from its lattice position, a defect is likely to form and the impinging ion reflects at an angle far from specular. Figure 6 shows an example of such an event in which the target atom leaves behind a surface vacancy.

The following picture may be envisioned to rationalize this finding. At very low energies, the ions do not penetrate very deep into the repulsive part of the surface potential. Far from the surface, the potential contours from individual surface atoms blend together, making the net potential appear nearly uniform. Momentum transfer to the surface is nonlocal—like a trampoline—and ions reflect specularly. At high energies, on the other hand, the ions penetrate deeper and begin to sense corrugation in the near-surface potential. Momentum transfer therefore becomes more local, involving only a few atoms that can be dislodged far from their lattice sites to form defects.

At intermediate ion energies near threshold, the picture becomes mixed. At low temperatures, surface atoms remain near their lattice sites so that ions reflect specularly. At higher temperatures, however, thermal vibrations of large amplitude begin to appear that degrade the instantaneous uniformity of the net potential. Ions that fortuitously impact such locations can wedge into the nonuniformities to transfer

momentum locally and thereby create defects. Thus temperature amplification in the *E-T* synergy arises because at some energy-dependent temperature, the uniformity in net potential degrades sufficiently to allow ion wedging. This temperature should scale with melting temperature, as observed in the simulations. The parameter σ is a measure of how fast the uniformity degrades as temperature increases. The value of σ for a given ion-surface system should depend upon the slope of the repulsive part of the ion-surface potential, together with the curvature of the potential between surface atoms near the bottom of the bonding well (since this curvature helps determine vibrational amplitude).

The picture described here need not be limited to noble gases impinging on Si or Ge. It is plausible to suppose that temperature-dependent threshold shifts characterize low-energy ion interactions with crystalline surfaces quite generally. In applications like IBAD or RIE, it may therefore be possible by judicious tuning of temperature and ion energy to exploit such threshold effects to select or deselect specific elementary rate processes. As mentioned earlier, the net behavior in such applications often represents a delicate balance among various elementary rates, so threshold-style nonlinearities offer an attractive means to choose among them. The angle of incidence may also play a role in temperature-dependent wedge effects and therefore serve as an additional tuning parameter, but the present investigation did not address this question.

This work was partially supported by the NSF (Grant Nos. CTS 98-06329 and CTS 02-03237). Z.W. acknowledges support of the DOE (Grant No. DEFG02-91ER45439) through the F. Seitz Materials Research Laboratory at UIUC. The authors thank Susanne Aref of the Statistics Department at UIUC for advice on the error analysis.

*Corresponding author. Electronic address: eseebaue@uiuc.edu

[1] J. E. Greene and S. A. Barnett, J. Vac. Sci. Technol. A **21**, 285 (1982).

[2] M. Nastasi, J. W. Mayer, and J. K. Hirvonen, *Ion-Solid Interactions: Fundamentals and Applications* (Cambridge University Press, New York, 1996).

[3] J. Heidberg, E. Kampshoff, R. Kuhnemuth, and O. Schonekas, Surf. Sci. **272**, 306 (1992).

[4] C. F. Abrams and D. B. Graves, J. Appl. Phys. **86**, 5938 (1999); J. Vac. Sci. Technol. A **18**, 411 (2000).

[5] For example, see S. Mohajerzadeh and C. R. Selvakumar, J. Appl. Phys. **81**, 3003 (1997).

[6] R. V. Stuart and G. K. Wehner, J. Appl. Phys. **33**, 2345 (1962).

[7] J. W. Rabalais, A. H. Al-Bayati, K. J. Boyd, D. Marton, J. Kulik, Z. Zhang, and W. K. Chu, Phys. Rev. B **53**, 10 781 (1996).

[8] S. M. Lee, C. J. Fell, D. Marton, and J. W. Rabalais, J. Appl. Phys. **83**, 5217 (1998).

[9] D. Marton, K. J. Boyd, and J. W. Rabalais, J. Vac. Sci. Technol. A **16**, 1321 (1998).

[10] B. W. Dodson, Nucl. Instrum. Methods Phys. Res. B **59/60**, 481 (1991).

[11] A. Kuronen, J. Tarus, and K. Nordlund, Nucl. Instrum. Methods Phys. Res. B **153**, 209 (1999).

[12] R. Ditchfield and E. G. Seebauer, Phys. Rev. Lett. **82**, 1185 (1999).

[13] R. Ditchfield and E. G. Seebauer, Phys. Rev. B **63**, 125317 (2001).

[14] B. K. Kellerman, J. A. Floro, E. Chason, D. K. Brice, S. T. Picraux, and J. W. White, J. Vac. Sci. Technol. A **13**, 972 (1995); J. Y. Tsao, E. Chason, K. M. Horn, D. K. Brice, and S. T. Picraux, Nucl. Instrum. Methods Phys. Res. B **39**, 72 (1989).

[15] M. V. Ramana Murty and H. A. Atwater, Phys. Rev. B **45**, 1507 (1992).

[16] R. A. Stansfield, K. Broomfield, and D. C. Clary, Phys. Rev. B **39**, 7680 (1989).

[17] L. A. Marqués, J. E. Rubio, M. Jaríz, L. A. Bailón, and J. J. Barbolla, J. Appl. Phys. **81**, 1488 (1997).

[18] M. Kitabatake and J. E. Greene, Thin Solid Films **272**, 271 (1996); J. Appl. Phys. **73**, 3183 (1993); M. Kitabatake, P. Fons, and J. E. Greene, J. Vac. Sci. Technol. A **9**, 91 (1991); **8**, 3726 (1990).

[19] C. E. Allen, R. Ditchfield, and E. G. Seebauer, Phys. Rev. B **55**, 13 304 (1997).

[20] F. H. Stillinger and T. A. Weber, Phys. Rev. B **31**, 5262 (1985).

[21] J. F. Ziegler, J. P. Biersack, and U. Littmark, *The Stopping and Range of Ions in Solids* (Pergamon Press, New York, 1985).